DALTON
FULL PAPER

The syntheses of metallomacrocycles containing unsymmetrical bridging ligands and the crystal structures of DL-[Mo{HB(3,5-$Me_2C_3HN_2)_3$}(NO)($OC_6H_4CH_2CH_2O$-4)]$_2$·2CH_2Cl_2 and DL-[W{HB(3,5-$Me_2C_3HN_2)_3$}(NO)($OC_6H_3NO_2$-4-CH_2CH_2O-3)]$_2$·CH_2Cl_2 †

Timothy E. Berridge, Matthew T. Barton, Thomas A. Hamor, Christopher J. Jones,* Ferida S. McQuillan, Keith Paxton and Natalie M. Rowley

School of Chemistry, University of Birmingham, Edgbaston, Birmingham, UK B15 2TT

Received 16th August 2000, Accepted 17th October 2000
First published as an Advance Article on the web 28th November 2000

Metallomacrocycles containing {M(NO)(Tp^{Me2})} [Tp^{Me2} = HB(3,5-$Me_2C_3HN_2)_3$; M = Mo or W] have been synthesized by direct reaction between [M(NO)(Tp^{Me2})I_2] and a heterotopic ligand HE–E′H {1,*x*-HOC_6H_4XOH (*x* = 3, X = CO; *x* = 3 or 4, X = CH_2 or CH_2CH_2)} in the presence of NEt_3. Only DL and *meso* isomers were isolated from the reactions where M = Mo, *x* = 4 and X = CO or CH_2CH_2 but both DL and *meso* and *syn* and *anti* isomers from the other reaction mixtures. Stereo-controlled synthetic routes to *syn* and *anti* isomers containing the $OC_6H_4CH_2O$-3 bridging ligand were developed through formation of [M(NO)(Tp^{Me2})(OC_6H_4CHO-3)]$_2$ (M = Mo or W) followed by reduction to [M(NO)(Tp^{Me2})($OC_6H_4CH_2OH$-3)]$_2$ and subsequent reaction with [M′(NO)(Tp^{Me2})I_2] (M′ = W or Mo) to give [{M(NO)(Tp^{Me2})}(μ-$OC_6H_4CH_2O$-3)$_2${M′(NO)(Tp^{Me2})}]. The trinuclear complex [{Mo(Tp^{Me2})(NO)}(μ-$OC_6H_4CH_2O$-3)$_2${W(Tp^{Me2})(NO)}$_2$(μ-1,3-OC_6H_4O)] was obtained from the reaction of [Mo(NO)(Tp^{Me2})($OC_6H_4CH_2OH$-3)]$_2$ with the binuclear complex [{W(NO)(Tp^{Me2})I}$_2$(μ-1,3-$O_2C_6H_4$)]. The crystal structures of DL-[Mo(Tp^{Me2})(NO)($OC_6H_4CH_2CH_2O$-4)]$_2$ and [W(Tp^{Me2})(NO)($OC_6H_3NO_2$-4-CH_2CH_2O-3)]$_2$ were established.

Introduction

The synthesis of novel metallomacrocyclic architectures through facile thermodynamically controlled self assembly reactions involving d^8, d^9 or d^{10} metal centres and polypyridyl ligands is now well established.[1–4] Numerous examples of bi-, tri- and higher nuclearity complexes are known, some of which exhibit host properties,[5] magnetism[6] or luminescence.[7] Metallomacrocycles derived from symmetric ditopic oxygen donor ligands are also known.[8–11] Earlier work by Maverick and co-workers demonstrated that ligands containing two β-diketonate binding sites could form metallomacrocycles containing planar copper(II) centres which display host properties.[9] Subsequently Saalfrank *et al*. showed that bicyclic structures could be obtained by combining ligands of this type with octahedral metal centres.[10] In these cases the robustness of the macrocycles arises, at least in part, from the kinetic stability of the metal–β-diketonate interaction. Monodentate metal–organo-oxide ligand interactions can also form a basis for metallomacrocycle formation. Stephan established the feasibility of constructing metallomacrocycles with ditopic ligands containing two monodentate alkoxide binding sites by synthesizing [Zr(η^5-$C_5H_5)_2${1,3-$(OCH_2)_2C_6H_4$}]$_2$.[8] In this case additional π bonding between the oxygen and the formally d^0 zirconium(IV) centres increases the stability of the metal–alkoxide bond and contributes to the robustness of the metallomacrocycle structure. In our own work[11] we have exploited the unusually strong bonding between the ligands RE^- (E = O, S or NH: R = hydrocarbyl) and the coordinatively unsaturated, formally d^4, metal centres in {M(Tp^{Me2})(NO)}$^{2+}$ {Tp^{Me2} = HB(3,5-$Me_2C_3HN_2)_3$} to form metallomacrocycles. Thus we have synthesized, and obtained the crystal structures of, the *syn* and *anti* isomers of [Mo(Tp^{Me2})(NO)(2,7-$O_2C_{10}H_6$)]$_2$,[11a] *syn*, *syn*-[Mo(Tp^{Me2})(NO)(1,4-$O_2C_6H_4$)]$_3$[11c] and *anti*, *syn*-[W(Tp^{Me2})(NO)(1,4-$O_2C_6H_4$)]$_3$,[11b] which contain rigid ditopic ligands. We have also synthesized and structurally characterised the *syn*- and *anti* isomers of [Mo(Tp^{Me2})(NO){1,4-$(OCH_2)_2C_6H_4$}]$_2$ and *anti*-[Mo(Tp^{Me2})(NO){(4-$OC_6H_4)_2CH_2$}]$_2$ which contain more flexible ditopic ligands.[11e] These compounds are formed under kinetic control and, in some cases, particular isomers are formed stereoselectively. All contain symmetrical bridging ligands which, in combination with octahedral {Mo(Tp^{Me2})(NO)} centres, lead to the availability of *syn*- or *anti*-isomeric forms for the binuclear species. In this paper we examine the formation of cyclophane like metallomacrocycles derived from [M(Tp^{Me2})(NO)I_2] (M = Mo or W) and the heteroditopic proligands[11e] HE–E′H {1,3-$HOC_6H_4CH_2OH$, 1,3-$HOC_6H_4CH_2CH_2OH$, 1,4-$HOC_6H_4CH_2CH_2OH$ or 1,3-$HOC_6H_4CO_2H$ (M = Mo)}. In principle the binuclear metallomacrocycle complexes formed, [M(Tp^{Me2})(NO)(E-E′)]$_2$, may exist as any of four isomers, DL, *meso*, *syn* or *anti* as shown in Fig. 1. Two synthetic approaches to such compounds have been examined. The first involves direct reaction of [M(Tp^{Me2})(NO)I_2] with a heteroditopic proligand,[11e] an objective of this part of the work being to establish whether such reactions show any stereoselectivity. The second approach offers a measure of stereochemical control through prior preparation of the achiral derivatives [M(Tp^{Me2})(NO)(OC_6H_4CHO-3)$_2$] which may be reduced to the alcohols [M(Tp^{Me2})(NO)($OC_6H_4CH_2OH$)$_2$] which can then serve as proligands in a subsequent metallomacrocycle forming reaction. Such metal containing ligands cannot be formed from the direct reaction of [M(Tp^{Me2})(NO)I_2] with $HOC_6H_4CH_2OH$ because the conditions necessary to induce substitution of both iodide ligands lead only to metallomacrocycle formation.

† Electronic supplementary information (ESI) available: NMR, IR and LSIMS spectroscopic data for complexes **1**–**31**. See http://www.rsc.org/suppdata/dt/b0/b006716o/

DOI: 10.1039/b006716o

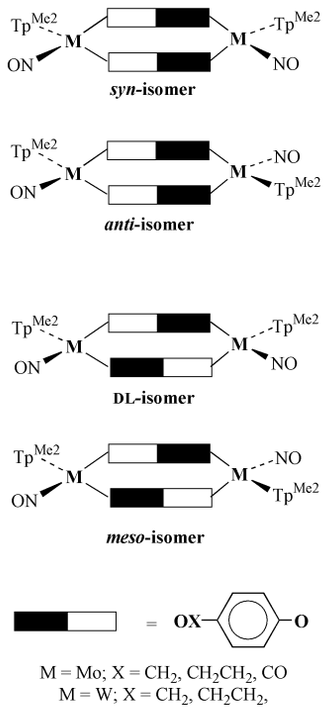

Fig. 1 Isomers of metallocyclophanes containing heterotopic bridging ligands.

Assuming that no ligand redistribution takes place, the reaction between $[M(Tp^{Me2})(NO)(OC_6H_4CH_2OH)_2]$ and $[M(Tp^{Me2})(NO)I_2]$ should then lead only to *syn* and *anti* isomers. The syntheses of these metal containing proligands offer new synthons for constructing redox active metallomacrocycles. The structural formulae of the new compounds reported here are presented in Figs. 2, 3 and 4.

Experimental

General details

All commercial reagents were used as supplied unless otherwise stated. The complexes $[M(Tp^{Me2})(NO)I_2]\cdot xC_6H_5Me$ [12] (M = Mo, $x = 1$; M = W, $x = 0$) were prepared using a previously reported method. Solvents used as reaction media were dried and freed of oxygen by standard methods. Reactions were carried out under a dinitrogen atmosphere but products were purified in air. Merck silica gel (60) was used as the stationary phase for column chromatography. Thin layer chromatography was carried out using Merck silica gel (60) F_{254} TLC plates. Infrared spectra were recorded as KBr pellets using a Perkin-Elmer 1600 series FT-IR spectrophotometer, 300 MHz ^{1}H NMR spectra using a Bruker AC 300 spectrometer, 400 MHz ^{1}H NMR spectra using a Bruker AMX 400 spectrometer, liquid secondary ion mass spectra (LSIMS) using a VG ZABSPEC mass spectrometer, and ESR spectra on a Bruker ESP 300 instrument. Cyclic voltammetry was carried out using an EG&G model 362 potentiostat and the Condecon 310 hardware/software package. Measurements were made using approximately 2×10^{-3} mol dm^{-3} solutions in dry dichloromethane under an atmosphere of nitrogen. A 0.2 mol dm^{-3} solution of $[Bu_4N][BF_4]$ was used as the base electrolyte. A platinum bead electrode was used and potentials were measured with reference to ferrocene used as an internal standard. UV/Vis spectra were obtained using a Perkin-Elmer λ3 spectrophotometer. Elemental analyses were carried out at the microanalytical laboratories, University of North London.

Syntheses

Synthetic procedures leading to crude products are presented below but details of compound purification by column chromatography, compound colours, eluents, R_f values, yields and elemental analyses are collected in Table 1. Spectroscopic data used for compound characterisation are deposited as Electronic Supplementary Information, Table S1.

$[Mo(Tp^{Me2})(NO)(OC_6H_4XO\text{-}3)]_n$ {X = CO, n = 2, 1; X = CH_2, n = 2, 2 and 3; X = CH_2CH_2, n = 2, 4, 5; n = 3, 8; $[Mo(Tp^{Me2})(NO)(OC_6H_4CH_2CH_2O\text{-}4)]_n$ {n = 2, 6 and 7; $[W(Tp^{Me2})(NO)(OC_6H_4XO\text{-}3)]_n$ (X = CH_2, n = 2, 9 and 10; X = CH_2CH_2, n = 2, 11, 12 and 13; n = 3, 14). To a round bottom flask containing $[M(Tp^{Me2})(NO)I_2]\cdot xC_6H_5Me$ (M = Mo: 0.5 g, 0.65 mmol. M = W: 0.5 g, 0.65 mmol) in toluene (50 ml), triethylamine (1 ml) was added and the mixture stirred. The bridging ligand HOC_6H_4XOH (X = CO, CH_2 or CH_2CH_2) (0.73 mmol) was then added and the mixture heated under reflux for fourteen hours, allowed to cool to room temperature, filtered and the solvent removed *in vacuo* to yield a crude solid which was purified using column chromatography.

$[W(Tp^{Me2})(NO)(OC_6H_4NO_2\text{-}4\text{-}CH_2CH_2O\text{-}3)]_2$, 15. This material was recovered from a solution of complexes **11** and **12** in $CDCl_3$ which had been used for an NMR measurement and was recrystallised from CH_2Cl_2–hexanes. Characterisation is based upon spectroscopic measurements and a single crystal X-ray diffraction study.

$[\{Mo(Tp^{Me2})(NO)I\}_2(OC_6H_4CH_2O\text{-}3)]$, 16 and $[Mo(Tp^{Me2})(NO)I(OC_6H_4CH_2OH\text{-}3)]$, 17. To a round bottom flask containing $[Mo(Tp^{Me2})(NO)I_2]\cdot C_6H_5Me$ (1 g, 1.30 mmol) in toluene (100 ml), 3-hydroxybenzyl alcohol (0.092 g, 0.74 mmol) was added and the mixture refluxed for six hours, allowed to cool to room temperature, filtered and the solvent removed *in vacuo* to yield a crude solid.

$[\{Mo(Tp^{Me2})(NO)I\}_2(OC_6H_4CH_2CH_2O\text{-}3)]$, 18 and $[Mo(Tp^{Me2})(NO)I(OC_6H_4CH_2CH_2OH\text{-}3)]$, 19. The procedure described for complexes **16** and **17** was followed using $[Mo(Tp^{Me2})(NO)I_2]\cdot C_6H_5Me$ (1 g, 1.30 mmol) and 2-(3-hydroxyphenyl)ethyl alcohol (0.102 g, 0.74 mmol).

$[\{Mo(Tp^{Me2})(NO)I\}_2(OC_6H_4CH_2CH_2O\text{-}4)]$, 20 and $[Mo(Tp^{Me2})(NO)I(OC_6H_4CH_2CH_2OH\text{-}4)]$, 21. The procedure described for complexes **16** and **17** was followed using $[Mo(Tp^{Me2})(NO)I_2]\cdot C_6H_5Me$ (1 g, 1.30 mmol) and 2-(4-hydroxyphenyl)ethyl alcohol (0.102 g, 0.74 mmol).

$[Mo(Tp^{Me2})(NO)(OC_6H_4CHO\text{-}3)_2]$, 22. To a round bottom flask containing $[Mo(Tp^{Me2})(NO)I_2]\cdot C_6H_5Me$ (2 g, 2.60 mmol) in toluene (250 ml), 3-hydroxybenzaldehyde (0.72 g, 5.92 mmol) and triethylamine (1 ml) were added and the mixture refluxed for twentyfour hours. It was allowed to cool to room temperature, filtered and the solvent removed *in vacuo* to yield a crude solid containing $[Mo(Tp^{Me2})(NO)(OC_6H_4CHO\text{-}3)_2]$.

$[Mo(Tp^{Me2})(NO)(OC_6H_4CH_2OH\text{-}3)_2]$, 23. $[Mo(Tp^{Me2})(NO)(OC_6H_4CHO\text{-}3)_2]$ (1 g, 1.5 mmol) was dissolved in dry, degassed methanol (150 ml) and to this $NaBH_4$ (0.23 g, 6 mmol) was added slowly. The mixture was then stirred at room temperature for twentyfour hours and the solvent removed *in vacuo* to yield a crude solid containing $[Mo(Tp^{Me2})(NO)(OC_6H_4CH_2OH\text{-}3)_2]$.

$[W(Tp^{Me2})(NO)(OC_6H_4CHO\text{-}3)_2]$, 24. $[W(Tp^{Me2})(NO)Cl_2]$ (0.5 g, 0.65 mmol) was treated with HOC_6H_4CHO-3 (0.16 g, 1.31 mmol) in refluxing toluene (100 ml) in the presence of triethylamine following the general procedure described above for **22** but with a reaction time of eight hours.

$[W(Tp^{Me2})(NO)(OC_6H_4CH_2OH\text{-}3)_2]$, 25. $[W(Tp^{Me2})(NO)(OC_6H_4CHO\text{-}3)_2]$ was reduced following the method described above for complex **23**.

***syn*- and *anti*-[{Mo(Tp^{Me2})(NO)}(OC$_6$H$_4$CH$_2$O-3)$_2${W(Tp^{Me2})(NO)}], 26 and 27.** To a round bottom flask containing [Mo(Tp^{Me2})(NO)(OC$_6$H$_4$CH$_2$OH-3)$_2$] (0.25 g, 0.37 mmol) in toluene (50 ml) and triethylamine (1 ml), [W(Tp^{Me2})(NO)I$_2$] (0.29 g, 0.37 mmol) was added and the mixture heated at 80 °C for fourteen hours. It was allowed to cool to room temperature, filtered, and the solvent removed *in vacuo* to yield a crude solid.

[{W(Tp^{Me2})(NO)}(OC$_6$H$_4$CH$_2$O-3)$_2${Mo(Tp^{Me2})(NO)}] 28. To a round bottom flask containing [W(Tp^{Me2})(NO)(OC$_6$H$_4$-CH$_2$OH-3)$_2$] (0.1 g, 0.13 mmol) in toluene (50 ml), [Mo(Tp^{Me2})-(NO)I$_2$]·C$_6$H$_5$Me (0.09 g, 0.12 mmol) was added along with triethylamine (1 ml). The mixture was refluxed for fourteen hours, allowed to cool to room temperature, filtered and the solvent removed *in vacuo*.

[{W(Tp^{Me2})(NO)I}$_2$(OC$_6$H$_4$O-3)], 29. To a round bottom flask containing [W(Tp^{Me2})(NO)I$_2$] (1 g, 1.3.1 mmol) in toluene (150 ml), resorcinol (0.7 g, 0.65 mmol) and triethylamine (1 ml) were added and the mixture was refluxed for 8 hours. It was then allowed to cool to room temperature, filtered and the solvent removed *in vacuo*.

[{Mo(Tp^{Me2})(NO)}(OC$_6$H$_4$CH$_2$O-3)$_2${W(Tp^{Me2})(NO)}$_2$-(OC$_6$H$_4$O-3)] 30 and 31. To a round bottom flask containing [{W(Tp^{Me2})(NO)I}$_2$(OC$_6$H$_4$O-3)] (130 mg, 0.1 mmol) in toluene (100 ml) and triethylamine (1 ml), [Mo(Tp^{Me2})(NO)(OC$_6$H$_4$-CH$_2$OH-3)$_2$] (63 mg, 0.1 mmol) was added and the mixture heated to 80 °C for fourteen hours. It was then allowed to cool to room temperature, filtered and the solvent removed *in vacuo*.

Crystallographic data [13]

Crystallization from dichloromethane–hexane afforded crystals of complexes **7** and **15** suitable for X-ray crystallographic studies. Cell dimensions and intensity data (Table 3) for the two complexes were measured on a Rigaku R-AXIS II area detector diffractometer. The structures were determined [13a] by direct methods and refined [13b] by least squares on F^2 using anisotropic thermal parameters for non-hydrogen atoms, apart from the carbon atoms of the dichloromethane in **15**, which were included in the calculations with isotropic thermal parameters. Hydrogen atoms were placed in calculated positions. Diagrams were drawn with ORTEP; [13c] thermal ellipsoids are at the 25% probability level.

CCDC reference number 186/2244.

See http://www.rsc.org/suppdata/dt/b0/b006716o/ for crystallographic files in .cif format.

Results and discussion

Synthetic studies

The direct reactions of [M(Tp^{Me2})(NO)I$_2$] with the heterotopic proligands HE–E′H involved heating the reagents under reflux in toluene for 14 hours in the presence of triethylamine. The reaction products were separated by column chromatography and characterised by IR and ^{1}H NMR spectroscopy, LSIMS and elemental analyses (Tables 1 and S1). The IR spectra of the new compounds contained a band in the region 2535 to 2595 cm^{-1} attributable to ν_{max}(BH), from the Tp^{Me2} ligand, together with a band in the region 1640 to 1665 (M = Mo) or 1610 to 1625 cm^{-1} (M = W) attributable to ν_{max}(NO). Molecular ions are present in the LSIMS spectra at the appropriate *m*/*z* value and elemental analyses are in accord with the formulations given. The ^{1}H NMR spectra were most useful in assigning structures to the compounds and allow chiral and achiral isomers of the binuclear complexes to be distinguished. In DL and *meso* isomers each metal centre is chiral and lacks a plane of symmetry but is indistinguishable by NMR spectroscopy from its companion. Thus the pyrazolyl C^4 protons of the Tp^{Me2} co-ligand should give rise to three signals in the area ratio 2:2:2 in the region δ 5.5 to 6.5. The protons of the pyrazolyl methyl groups should appear as six signals in the area ratio 6:6:6:6:6:6 in the region δ 1.9 to 3. In the *syn* and *anti* isomers each metal centre is bisected by a centre of symmetry so that, as two non-equivalent metal centres are present, the ^{1}H NMR spectra should contain four signals attributable to the pyrazolyl C^4 protons in the area ratio 2:1:2:1. The pyrazolyl methyl protons should appear as eight signals in the area ratio 6:3:6:3:6:3:6:3. Although some signal overlap may occur, for the binuclear complexes the ^{1}H NMR signals due to the Tp^{Me2} ligand are usually sufficiently well resolved to allow unambiguous assignment of the isomer type. Earlier studies [11] have shown that the *syn* and *anti* isomers of binuclear metallomacrocycles containing symmetric ditopic ligands give rise to significantly different ^{1}H NMR spectra. Thus, although the ^{1}H NMR spectra of the *syn* and *anti* isomers, or the DL and *meso* isomers, do not provide a basis for determining which of each pair is which, the different isomers in each pair should nonetheless give rise to different spectra.

The reaction between [Mo(Tp^{Me2})(NO)I$_2$] and 1,3-HOC$_6$H$_4$CO$_2$H afforded [Mo(Tp^{Me2})(NO)(1,3-OC$_6$H$_4$CO$_2$)]$_2$, **1**, in 37% yield (Fig. 2). The ^{1}H NMR spectrum (ESI Table S1) is consistent with the presence of a single isomer, either the DL or *meso* form. As no other binuclear isomers could be isolated from the reaction mixture it appears that the reaction is stereoselective. The IR spectrum of **1** is unusual in that ν_{max} (BH) appears at 2593 cm^{-1} rather than the more typical value of *ca.* 2545 cm^{-1}. The value of 1663 cm^{-1} observed for ν_{max}(NO) is slightly higher than the 1656 cm^{-1} found for [Mo(Tp^{Me2})-(NO)(OPh)$_2$] and consistent with the carboxylate group being a poorer π-donor than a second phenoxide ligand. A band attributable to ν_{max} (CO) is observed at 1693 cm^{-1}.

A reaction between [Mo(Tp^{Me2})(NO)I$_2$] and the structurally similar ligand 1,3-HOC$_6$H$_4$CH$_2$OH afforded two fractions containing the binuclear metallomacrocycle [Mo(Tp^{Me2})(NO)-(1,3-OC$_6$H$_4$CH$_2$O)]$_2$. The ^{1}H NMR spectrum (ESI Table S1) of the first, **2**, obtained in 24% yield, is consistent with its formulation as the DL or *meso* isomer and that of the second, **3**, obtained in only 3% yield, with its formulation as the *syn* or *anti* isomer. This reaction appears to be stereoselective in that, in the products isolated, the DL or *meso* isomer predominates over the *syn* or *anti* isomer by a factor of about 7 to 1. The effect of lengthening the bridging ligand by one CH$_2$ unit was investigated by carrying out a reaction with 1,3-HOC$_6$H$_4$CH$_2$CH$_2$OH. Two binuclear fractions were again isolated but in this case similar yields of each were obtained. The first, **4**, obtained in 19% yield, is shown by ^{1}H NMR spectroscopy to contain the DL or *meso* isomer whilst the second, **5** obtained in 13% yield, is found to contain the *syn* or *anti* isomer. A further experiment was carried out to determine the effect of changing the orientation of the substituents on the aryl group of the heteroditopic ligand by using 1,4-HOC$_6$H$_4$CH$_2$CH$_2$OH. In this case two binuclear fractions were again obtained, **6**, in 12% yield, and **7**, in 14% yield, in addition to a trinuclear fraction, **8**, in 9% yield. The ^{1}H NMR spectra of **6** and **7** show that both are either the DL or *meso* isomer but do not distinguish which is which. However, a crystal structure of **7** (see below) establishes that this compound is the DL isomer so that **6** must then be the *meso* isomer. The ^{1}H NMR spectrum of **8** is complicated by extensive signal overlap arising from the presence of a number of isomers (Fig. 2), there being six pairs of enantiomers arising from the various ways of arranging the three bridging ligands and three nitric oxide ligands. Despite this the relative areas of the groups of signals due the protons associated with the Tp^{Me2} ligand and the OC$_6$H$_4$CH$_2$CH$_2$O ligand are in accord with the formulation of **8** as a cyclic oligomer [Mo(Tp^{Me2})(NO)(OC$_6$H$_4$CH$_2$CH$_2$O)]$_n$ and a molecular ion appears at *m*/*z* = 1678 in the LSIMS indicating a value of *n* = 3.

The reactions of [W(Tp^{Me2})(NO)I$_2$] with the heterotopic ligands were also investigated and characterisable products

Table 1 Purification procedures and elemental analyses

Complex	Eluent[a] Colour	R_f[b]	Yield mg (%)	Found (Calc.) (%) C	H	N
1	CH_2Cl_2 Brown	0.35	132 (37)	47.5 (47.2)	5.12 (4.65)	15.3 (15.5)
2	7 : 3 v/v CH_2Cl_2–C_6H_{14} Brown	0.67	86 (24)	48.9 (48.4)	5.19 (5.14)	18.0 (18.0)
3	7 : 3 v/v CH_2Cl_2–C_6H_{14} Brown	0.52	11 (3)	48.7 (48.4)	5.32 (5.14)	18.0 (18.0)
4	6 : 4 v/v CH_2Cl_2–C_6H_{14} Brown	0.34	66 (19)	49.6 (49.4)	5.44 (5.34)	17.3 (17.5)
5	6 : 4 v/v CH_2Cl_2–C_6H_{14} Brown	0.28	46 (13)	49.2 (49.4)	5.39 (5.34)	17.6 (17.5)
6	6 : 4 v/v CH_2Cl_2–C_6H_{14} Brown	0.44	41 (12)	49.4 (49.4)	5.46 (5.34)	17.7 (17.5)
7	6 : 4 v/v CH_2Cl_2–C_6H_{14} Brown	0.31	50 (14)	49.6 (49.4)	5.46 (5.34)	17.4 (17.5)
8	6 : 4 v/v CH_2Cl_2–C_6H_{14} Brown	0.22	33 (9)	49.2 (49.4)	5.26 (5.34)	17.3 (17.5)
9	9 : 1 v/v CH_2Cl_2–C_6H_{14} Orange	0.53	19 (5)	41.7 (41.7)	4.59 (4.42)	15.4 (15.5)
10	9 : 1 v/v CH_2Cl_2–C_6H_{14} Orange	0.17	22 (5)	41.8 (41.7)	4.34 (4.42)	15.3 (15.5)
11	9 : 1 v/v CH_2Cl_2–C_6H_{14} Orange	0.45	36 (6)	42.3 (42.7)	4.82 (4.64)	15.4 (15.2)
12	9 : 1 v/v CH_2Cl_2–C_6H_{14} Orange	0.43	13 (3)	42.9 (42.7)	4.51 (4.64)	15.1 (15.2)
13	9 : 1 v/v CH_2Cl_2–C_6H_{14} Orange	0.30	16 (4)	42.3 (42.7)	4.91 (4.64)	15.5 (15.2)
14	9 : 1 v/v CH_2Cl_2–C_6H_{14} Orange	0.35	36 (9)	42.6 (42.7)	4.76 (4.64)	15.2 (15.2)
15[c]	9 : 1 v/v CH_2Cl_2–C_6H_{14} Pink	0.42	12 (3)	—	—	—
16	7 : 3 v/v CH_2Cl_2–C_6H_{14} Purple	0.8	134 (17)	36.5 (36.3)	4.02 (4.09)	16.2 (16.0)
17	7 : 3 v/v CH_2Cl_2–C_6H_{14} Purple	0.2	256 (30)	39.1 (39.2)	4.33 (4.31)	14.4 (14.6)
18	7 : 3 v/v CH_2Cl_2–C_6H_{14} Purple	0.82	97 (13)	36.9 (36.9)	4.23 (4.21)	15.8 (15.9)
19	7 : 3 v/v CH_2Cl_2–C_6H_{14} Purple	0.27	152 (17)	40.0 (40.2)	4.54 (4.51)	14.3 (14.3)
20	7 : 3 v/v CH_2Cl_2–C_6H_{14} Purple	0.78	153 (20)	37.0 (36.9)	4.28 (4.21)	15.6 (15.9)
21	7 : 3 v/v CH_2Cl_2–C_6H_{14} Purple	0.31	426 (49)	39.8 (40.2)	4.52 (4.51)	14.2 (14.3)
22	98 : 2 v/v CH_2Cl_2–THF Brown	0.72	1360 (79)	52.5 (52.4)	5.20 (4.85)	14.7 (14.7)
23	95 : 5 v/v CH_2Cl_2–THF Brown	0.64	820 (82)	52.1 (52.0)	5.28 (5.42)	14.7 (14.7)
24	CH_2Cl_2 Brown	0.40	135 (27)	46.3 (46.2)	4.11 (4.28)	12.8 (13.0)
25	7 : 3 v/v CH_2Cl_2–THF Brown	0.38	207 (42)	—	—	—

Table 1 (*contd.*)

Complex	Eluent[a] Colour	R_f[b]	Yield mg (%)	Found (Calc.) (%) C	H	N
26	8:2 v/v CH_2Cl_2–C_6H_{14} Dark yellow	0.34	110 (25)	44.9 (44.8)	4.85 (4.75)	16.5 (16.6)
27	8:2 v/v CH_2Cl_2–C_6H_{14} Dark yellow	0.18	21 (5)	44.9 (44.8)	4.64 (4.75)	16.7 (16.6)
28	8:2 v/v CH_2Cl_2–C_6H_{14} Brown	0.41	34 (25)	44.7 (44.8)	4.82 (4.75)	16.6 (16.6)
29	9:1 v/v CH_2Cl_2–C_6H_{14} Purple	0.76	138 (18)	31.3 (31.2)	3.26 (3.47)	14.1 (14.2)
30	CH_2Cl_2 Brown	0.44	35 (21)	43.9 (43.4)	4.62 (4.56)	16.2 (16.4)
31	CH_2Cl_2 Brown	0.32	28 (17)	43.8 (43.4)	4.58 (4.56)	16.4 (16.4)

[a] THF = tetrahydrofuran. [b] Obtained with the specified eluent on Merck silica gel (60) F_{254} TLC plates. [c] Recovered from a $CDCl_3$ solution used for a NMR measurement and characterised by a single crystal X-ray diffraction study.

obtained in two cases, although in lower yield than for the reactions involving $[Mo(Tp^{Me2})(NO)I_2]$. The reaction with 1,3-$HOC_6H_4CH_2OH$ afforded two binuclear fractions, **9** and **10**, each in 5% yield. The ^{1}H NMR spectra indicate that **9** is a mixture of DL and *meso* isomers and **10** a mixture of *syn* and *anti* isomers. Attempts to separate these isomer mixtures by column chromatography were unsuccessful.

The reaction of $[W(Tp^{Me2})(NO)I_2]$ with 1,3-HOC_6H_4-CH_2CH_2OH afforded three binuclear fractions **11**, in 6% yield, **12**, in 3% yield, and **13,** in 4% yield in addition to a trinuclear fraction **14**, in 9% yield. The ^{1}H NMR spectrum of **11** showed no plane of symmetry to be present in the Tp^{Me2} ligands, indicating that the DL or *meso* isomer had been isolated. The spectra of **12** and **13** differed but each showed the presence of a plane of symmetry in the Tp^{Me2} ligands establishing that the *syn* and *anti* isomers had been isolated, although the spectra do not distinguish which compound is which isomer. The formulation of **14** as a cyclic trimer $[W(Tp^{Me2})(NO)(OC_6H_4CH_2CH_2O)]_3$ is supported by the LSIMS data and the relative areas of the groups of ^{1}H NMR signals due the protons associated with the Tp^{Me2} ligand and the $OC_6H_4CH_2CH_2O$ ligand. However, as is the case with the trinuclear complex **8**, the ^{1}H NMR spectrum of **14** is complicated by signal overlap due to the presence of a number of different isomers.

During initial attempts to separate complexes **11** and **12** by recrystallisation from acetone–hexane mixtures, a pink product, **15**, crystallised from a solution of **11** and **12** which had been recovered from an NMR measurement. The formulation is based on ^{1}H NMR and IR spectroscopy, LSIMS and a single crystal X-ray analysis (see below). The ^{1}H NMR spectrum indicated that the 4-position protons of the aryl ring in the bridging ligand had been substituted but the nature of the substituent was not apparent, no new signals appearing in place of the substituted protons. However, the relative areas of the signals were consistent with the presence of a cyclic oligomer of formula $[W(Tp^{Me2})(NO)(OC_6H_3(Y)CH_2CH_2O)]_n$. The LSIMS spectrum contains a molecular ion at *m*/*z* 1385, 90 units greater than expected for the unsubstituted macrocyclic dimer, with no other significant ions being observed above *m*/*z* 511. This would suggest that **15** is binuclear with Y having a mass of 46, consistent with it being either a carboxylic acid or a nitro group. The IR spectrum contains bands attributable to ν(BH) at 2550 cm^{-1} and ν(NO) (nitrosyl) at 1623 cm^{-1}. However, no bands are observed in the region 1600 to 1700 cm^{-1} which might be attributed to ν(OH) or ν(C=O) although a band present at 1572 cm^{-1} could be due to ν(NO) arising from the presence of an aryl nitro group. This formulation also gives the best fit to the X-ray data (see Table 5). The origin of the nitro group is unclear. As the sample was recovered from an NMR tube it is possible that a tube contaminated with nitric acid from cleaning had been used and this had led to nitration of the complex either directly or through the presence of NO_2 in the tube. However, attempts to reproduce this reaction failed leaving the complex either unchanged or decomposed. There was no evidence that the starting materials used to form the original complex were nitrated. The structure determination of **15** shows it to be the DL isomer so that, assuming **15** is derived from **11** without ligand redistribution, this would imply that **11** is also a DL isomer.

Although the direct reactions between heteroditopic ligands and $[M(Tp^{Me2})(NO)I_2]$ (M = Mo or W) offer the simplest synthetic approach to the metallomacrocycles described above, alternative stepwise syntheses are also possible. Three such routes to binuclear metallomacrocycles may be proposed. The first is based on the preparation, as intermediates, of monosubstituted complexes $[M(Tp^{Me2})(NO)I(E–E'H)]$ which may react further with the elimination of 2HI to form $[M(Tp^{Me2})(NO)(E–E')]_2$. The second involves formation of a binuclear intermediate $[\{M(Tp^{Me2})(NO)I\}_2(E–E')]$ which may be treated with further HE–E′H. The third route involves the preparation of a bis-substituted complex $[M(Tp^{Me2})(NO)$-$(E–E'H)_2]$ which may be treated further with $[M(Tp^{Me2})(NO)I_2]$.

Samples of the bimetallic complexes $[\{Mo(Tp^{Me2})(NO)$-$I\}_2\{OC_6H_4(CH_2)_nO$-$z\}]$ **16** ($n = 1$, $z = 3$), **18** ($n = 2$, $z = 3$), **20** ($n = 2$, $z = 4$) and monometallic complexes $[Mo(Tp^{Me2})(NO)$-$I\{OC_6H_4(CH_2)_nOH$-$z\}]$ **17** ($n = 1$, $z = 3$), **19** ($n = 2$, $z = 3$) and **21** ($n = 2$, $z = 4$) were prepared following previously established procedures and characterised.[14,15] However, attempts to prepare the corresponding mononuclear bis(aryl oxide) complexes $[M(Tp^{Me2})(NO)\{OC_6H_4(CH_2)_nOH$-$z\}_2]$ were unsuccessful since the conditions necessary to form the intermediate led directly to metallomacrocycle formation. Instead, it proved possible to prepare the di-substituted complexes $[M(Tp^{Me2})(NO)$-$(OC_6H_4CH_2OH$-$3)_2]$ (M = Mo or W) by reduction of the formylphenoxide complexes $[M(Tp^{Me2})(NO)(OC_6H_4CHO$-$3)_2]$. Thus $[Mo(Tp^{Me2})(NO)(OC_6H_4CHO$-$3)_2]$ **22** was prepared then reduced using $NaBH_4$ to afford $[Mo(Tp^{Me2})(NO)(OC_6H_4$-$CH_2OH$-$3)_2]$, **23**. A similar procedure afforded $[W(Tp^{Me2})$-$(NO)(OC_6H_4CHO$-$3)_2]$ **24** and $[W(Tp^{Me2})(NO)(OC_6H_4CH_2OH$-$3)_2]$, **25**, which were characterised by their IR, LSIMS and ^{1}H NMR spectra, all of which were unremarkable and in accord with their formulations. These proligands could then be used to prepare heterobinuclear complexes. Thus **23** reacted with $[W(Tp^{Me2})(NO)I_2]$ to form two isomers of a binuclear complex,

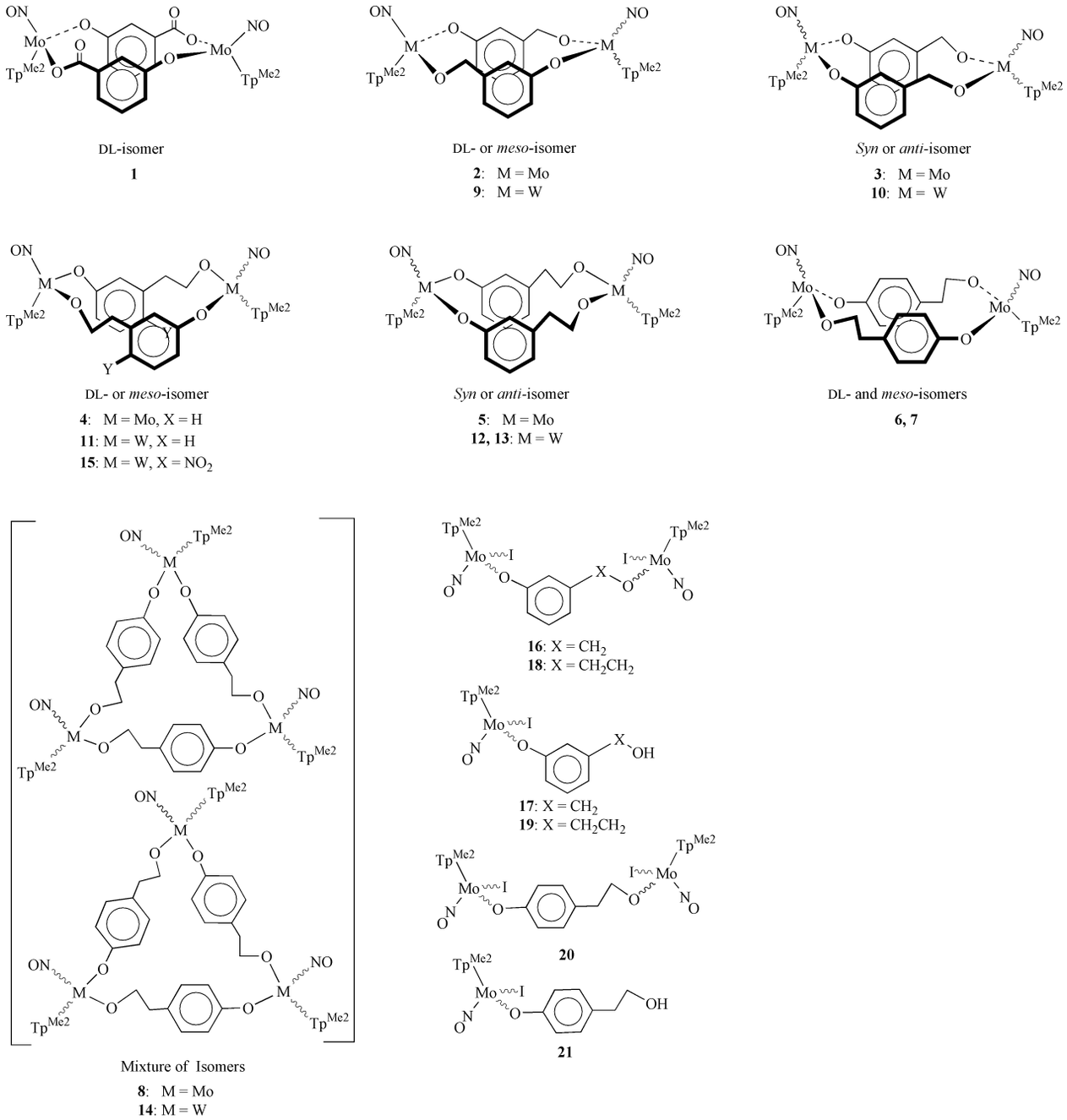

Fig. 2 Structural formulae for compounds **1** to **21**.

26 and **27**, whilst the reaction of **25** with $[Mo(Tp^{Me2})(NO)I_2]$ afforded **28** (Fig. 3). Similarly the reaction of **23** with the binuclear complex $[\{W(Tp^{Me2})I(NO)\}_2(1,3\text{-}O_2C_6H_4)]$, **29**, afforded a trinuclear complex isolated in two forms, **30** and **31** (Fig. 4).

The overall yields of macrocycles obtained using the stepwise approach are generally lower than those obtained from direct reaction of the proligand with $[Mo(Tp^{Me2})(NO)I_2]$. However, the variations in yields do not allow any one particular route to be identified as the most efficient for macrocycle formation. The yields obtained from the direct reactions of $[Mo(Tp^{Me2})(NO)I_2]$ with HE–E′H are generally higher after 24 than 4 hours, and the *syn* or *anti* isomers do not readily convert into the DL or *meso* isomers.

Electronic spectra and electrochemical studies

The electronic spectra of the new complexes are summarised in Table 2 and are in keeping with previous observations.[16] Absorptions in the region 389–405 nm can be attributed to the ditopic ligand to M (Mo or W) Ligand to Metal Charge Transfer (LMCT), absorptions in the regions 288–273 and 346–342 nm are assigned to (NO) to Mo and (NO) to W LMCT respectively and finally the strongest absorption in the region 239–224 nm has been assigned to Tp^{Me2} π–π* transitions.

The electrochemical properties of the new macrocyclic complexes were investigated using cyclic voltammetry and the results obtained are summarised in Table 2. Earlier electrochemical studies of acyclic binuclear complexes[15] containing $\{M(Tp^{Me2})(NO)\}^{2+}$ centres linked by symmetric bridging ligands have revealed interactions between the metal centres which vary with the nature of the bridging ligand. More recent electrochemical studies of metallomacrocycles[11] have shown similar effects and extended the series to include tri- and tetranuclear compounds.[11d] The electrochemical properties of binuclear metallomacrocycles containing asymmetric bridging ligands E–E′ will be affected by both the nature and the relative orientation within the complex of E–E′. Typically aryloxy complexes $[Mo(Tp^{Me2})(NO)(OAr)_2]$ (Ar = aryl)[17] undergo one-electron reductions at more positive potentials than their alkoxide containing counterparts $[Mo(Tp^{Me2})(NO)(OR)_2]$

(R = alkyl).[14,18] Thus the *syn* or *anti* isomers of complexes containing $OC_6H_4(CH)_nO$ ($n = 1$ or 2) bridges should exhibit two reduction waves, one associated with the bis(aryloxy) substituted metal centre and the other, at more negative potential, with the bis(alkoxy) substituted metal centre. In the case of the DL or *meso* isomers both metal centres are equivalent and should reduce at the same potential, intermediate between those of bis(aryloxy) and bis(alkoxy) substituted metal centres.

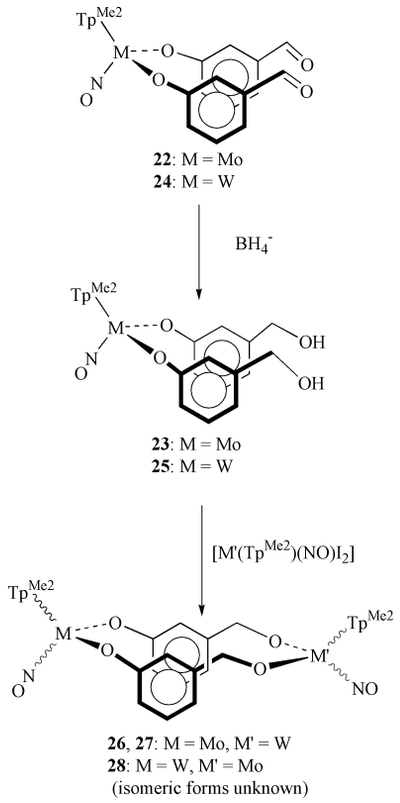

Fig. 3 The stepwise formation of *syn* or *anti* isomers of binuclear metallocyclophanes and the structural formulae of compounds **22** to **28**.

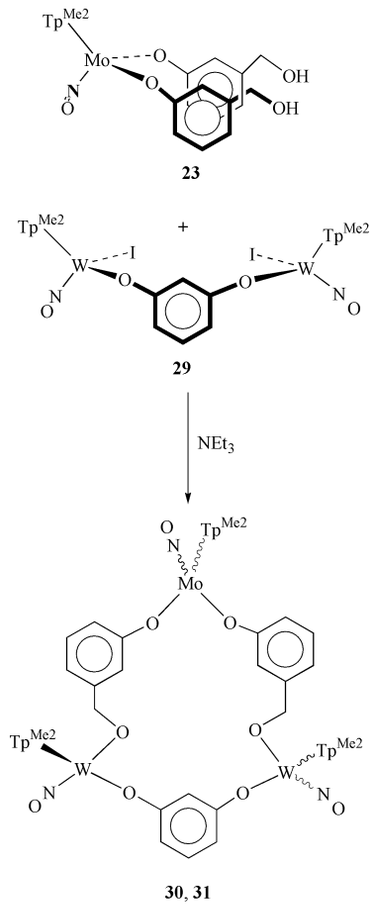

Fig. 4 The stepwise formation of a trinuclear metallocyclophane and the structural formulae of compounds **29** to **31**.

Table 2 Electronic spectra and electrochemistry of metallomacrocycles

Complex	λ/nm (ε/dm^3 mol^{-1} cm^{-1})[a,b]	E_f^c/V	ΔE_p^d/mV	i_a/i_c^e
1	429 (774), 288 (1875), 224 (9761)	−0.62	540	1.1
2	390 (840), 273 (1874), 235 (3583)	−1.02	90	1
		−1.17	90	1.0
3	404 (529), 273 (1354), 227 (4051)	−0.67	103	1
		−1.4	80	0.9
4	389 (643), 273 (2033), 235 (3715)	−1.02	180	1.0
5	406 (826), 274 (1889), 228 (3249)	−0.81	220	1.0
		−1.33	130	1.05
6	405 (895), 272 (1467), 230 (3733)	—	—	—
7	405 (667), 273 (1250), 228 (4247)	−1.09	260	1.0
8	414 (1416), 273 (3123), 227 (10956)	−1.03	110	1.0
9	326 (960), 226 (4584)	−1.53	100	1
		−1.68	100	1.1
10	337 (876), 234 (4245)	−1.21	150	1.0
11	326 (789), 239 (5014)	−1.61	220	1.0
12	332 (929), 234 (5002)	−1.28	130	1.0
13	342 (918), 239 (4410)	−1.28	130	0.8
14	343 (1764), 228 (9974)	−1.29	270	1.1
26	404 (814), 237 (4460), 227 (6160)	−0.68	240	1.0
27	416 (590), 235 (3900), 225 (3890)	−0.73	385	1.0
28	349 (1413), 238 (5831), 228 (6644)	−1.24	110	1.0
		−1.48	150	1.0
30	332 (1330), 234 (5800), 226 (11136)	−0.72	205	1.1
31	328 (1150), 239 (4998), 227 (9958)	−0.74	200	1.0

[a] Concentrations *ca.* 1×10^{-5} mol dm^{-3}. [b] Measurements from solutions in dichloromethane. [c] Formal electrode potential measured from cyclic voltammograms obtained under an inert atmosphere at a platinum bead electrode from *ca.* 10^{-3} mol dm^3 solutions in dry CH_2Cl_2 containing 0.2 mol dm^{-3} $[Bu_4N][BF_4]$ as the supporting electrolyte. Potentials were measured *vs.* a saturated calomel reference electrode with ferrocene (Fc) added as an internal standard. Under these conditions E_f for the Fc–Fc$^+$ couple was 0.56 ± 0.01 V. [d] Difference between cathodic and anodic peak potentials. Software compensation for the internal cell resistance was made in each case. [e] Ratio of anodic to cathodic peak currents.

The partly saturated nature of most of the bridging ligands used here suggests that only weak interactions between the metal centres should be present.

The electrochemistry of complex **1** was in keeping with its formulation as a DL isomer containing two equivalent weakly interacting metal centres. The cyclic voltammogram contained two unresolved waves at *ca.* −0.62 V (CH_2Cl_2 *vs.* SCE) but the two reduction processes could be resolved in the first and second derivative plots giving cathodic peak potentials at −0.570 and −0.799 V. The peak separation of 229 mV indicates that some metal–metal interaction is present, mediated by the $OC_6H_4CO_2$-3 bridging ligands and the cyclic voltammogram suggests that they are chemically reversible.

The cyclic voltammogram of the molybdenum complex **2**, derived from 3-hydroxybenzyl alcohol, contained two reversible waves at −1.02 and −1.17 V. These reduction potentials lie between those of bis(aryloxy) and bis(alkyloxy) molybdenum complexes,[14,17,18] in accord with the formulation of the complex as the DL or *meso* isomer, but the observation of two waves suggests that a weak metal–metal interaction is supported by the bridging ligand. The tungsten complex **9** shows two chemically reversible waves at −1.53 and −1.68 V. Bearing in mind that tungsten complexes of this type typically reduce at potentials *ca.* 450 mV more negative than their molybdenum containing counterparts,[17] **9** and **2** show very similar electrochemical behaviour. The cyclic voltammogram of **3** contains two chemically reversible waves at −0.67 and −1.4 V consistent with its formulation as a *syn* or *anti* isomer containing one bis(aryloxy) and one bis(alkoxy) bonded molybdenum centre. The related tungsten complex **10** shows only a single chemically reversible wave at −1.21 V. This may be attributed to the reduction of a bis(aryloxy) tungsten centre by comparison with [{W(Tp^{Me2})(NO)}$(OPh)_2$] which has E_f = −1.20 V (MeCN *vs.* SCE).[17] A second wave corresponding to reduction of the bis(alkoxy) tungsten centre should be present but was not observed, presumably because the reduction potential lies beyond the solvent limit for the conditions used (−1.8 V).

The DL or *meso* isomer of the molybdenum complex containing the $OC_6H_4CH_2CH_2O$-3 ligand, **4**, shows only a single chemically reversible wave at −1.02 V. The large ΔE_p value of 180 mV indicates some electrochemical irreversibility and a similar situation is observed for the DL or *meso* isomer of the tungsten complex **11**. A single chemically reversible wave is observed at −1.61 V; the value of ΔE_p is again very large at 220 mV. These potentials lie between those expected for the corresponding bis(aryloxy) and bis(alkyloxy) complexes in accord with the formulations of **4** and **11** as DL or *meso* isomers. The cyclic voltammogram of the *syn* or *anti* isomer, **5**, contained two chemically reversible waves at −0.81 and −1.33 V with ΔE_p values of 220 and 130 mV respectively, in accord with the presence of both bis(aryloxy) and bis(alkoxy) molybdenum centres. However, the related tungsten complexes **12** and **13** each show only a single wave at −1.28 V as found for **10**. Owing to its poor solubility no satisfactory electrochemical data could be obtained for **6**. The other molybdenum complexes derived from 2-(4-hydroxyphenyl)ethyl alcohol exhibit single broad, apparently chemically reversible, waves. These are observed at −1.09 V for the cyclic dimer, **7**, and −1.03 V for the cyclic trimer, **8**. In the cyclic voltammogram of the tungsten containing cyclic trimer **14** a single chemically reversible wave was observed at −1.29 V.

The cyclic voltammogram of the mixed molybdenum and tungsten complex **26** only shows a single wave at −0.68 V (SCE *vs.* CH_2Cl_2) which can be assigned to reduction of the bis(aryloxy) molybdenum(II) centre, similarly a single wave is observed for the isomeric complex **27** at −0.73 V. It is thought that the second wave corresponding to reduction of the bis(alkoxy) bound tungsten centre appears at too negative a potential to be observed under the experimental conditions used. Despite changing the solvent to tetrahydrofuran in order to increase the range of potentials accessible to −2.0 V no second wave was observed. For both **26** and **27** the very large ΔE_p values obtained indicate a large degree of electrochemical irreversibility, although the i_a/i_c values suggest that the reductions are chemically reversible. Also of note is the difference in molybdenum reduction potential between **26** and **27**, with **27** being reduced at a potential 50 mV more negative than **26**. This would suggest the conformation adopted by **26** allows for better orbital correlation between the ditopic ligand filled oxygen p orbitals and vacant metal d orbitals. This would also result in the ν(NO) in the IR spectrum of **26** shifting to lower frequency due to increased π retrodonation into the nitrosyl empty π* orbital. This is indeed observed with the ν(NO) of **26** being 10 cm^{-1} lower than that of **27**. The observed cyclic voltammogram of **28** contains two reversible waves at −1.24 and −1.48 V. Based on electrochemical data obtained from the analogous homometallic molybdenum and tungsten complexes it is possible to assign the two waves with some confidence. The tungsten complex **10** showed a single wave at −1.21 V assigned to the reduction of the bis(aryloxy) tungsten centre. It would seem reasonable to assign the reduction at −1.24 V for **28** to a similar process. Likewise the electrochemistry of the related molybdenum complex **3** contained two waves, the second at −1.4 V being assigned to the reduction of the bisalkoxy molybdenum centre. Again the wave observed for **28** at −1.48 V would seem consistent with a similar reduction process associated with a bis(alkoxy) substituted $\{Mo(Tp^{Me2})(NO)\}^{2+}$ centre. Both waves are chemically reversible but the large ΔE_p values indicate kinetically slow electron transfer. The cyclic voltammograms for **30** and **31** are essentially the same and show only single reversible reduction processes at −0.72 and −0.74 V respectively. These E_f values are consistent with the reduction of a bis(aryloxy) molybdenum centre. The two tungsten centres might be expected to show a one electron reduction at around −1.53 V followed by a second one electron reduction shifted to more negative potential by approximately 200 mV due to metal–metal interaction across the resorcinol bridge. However, no electrochemical processes are observed in this region. It may be that prior reduction of the molybdenum centre causes the tungsten reduction potentials to shift beyond the solvent limit.

Structural studies

Views of complexes **7** and **15** are shown in Figs. 5 and 6, and selected geometric parameters are listed in Tables 4 and 5. The nitrosyl substituents are oriented *syn* with respect to each other in both complexes. The coordination geometry at the metal atoms is approximately octahedral in each case. The mean deviations from ideal octahedral range from 7.3 to 7.9°. As had been noted previously,[11a,e] these deviations show a consistent pattern and differences between corresponding angles at the four metal centers are relatively small, mean differences 0.8–1.9°, with no apparent distinction between molybdenum and tungsten. Comparison of these with data for analogous monomeric[11f,g] complexes shows that the mean differences between corresponding angles are of similar magnitude. The metal–oxygen bonds fall into two categories. Where the oxygen links the metal to an sp^3-hybridised carbon, the Mo–O bonds have lengths 1.893 and 1.897 Å, W–O 1.873 and 1.888 Å, whereas in the M–O–C(sp^2) system the M–O lengths are longer, Mo–O 1.929 and 1.919, W–O 1.942 and 1.944 Å. Both categories of Mo–O bonds are relatively short. This implies p_π–d_π electron donation from the donor atom (O) to the coordinatively unsaturated metal. Large angles at oxygen and the small N(nitrosyl)-M–O–C torsion angles (<±19.5°) are consistent with this, although steric effects may also play a role in increasing the bond angle at oxygen. The longer M–O lengths in systems where the carbon atom is unsaturated may be the result of additional electron delocalisation involving the aromatic

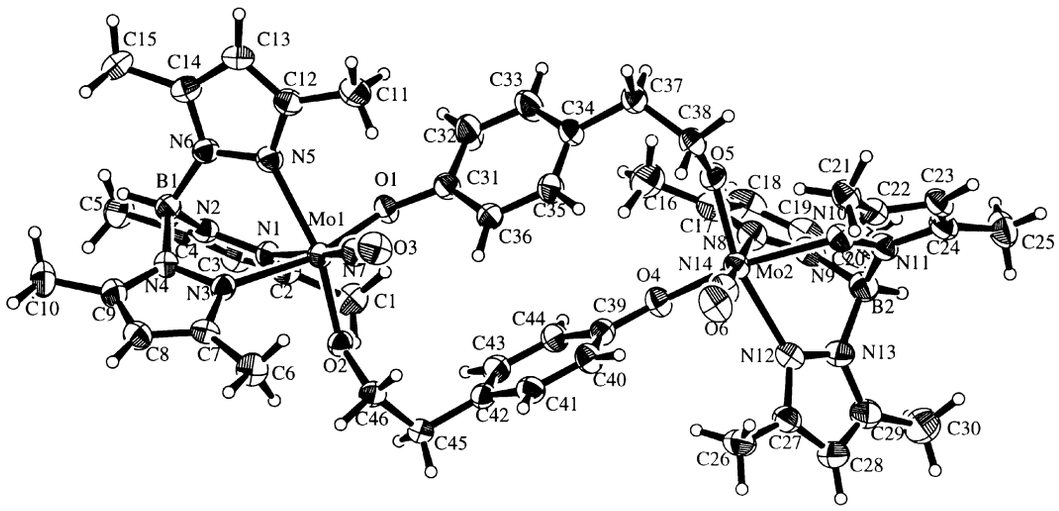

Fig. 5 A view of complex **7** showing the atom numbering.

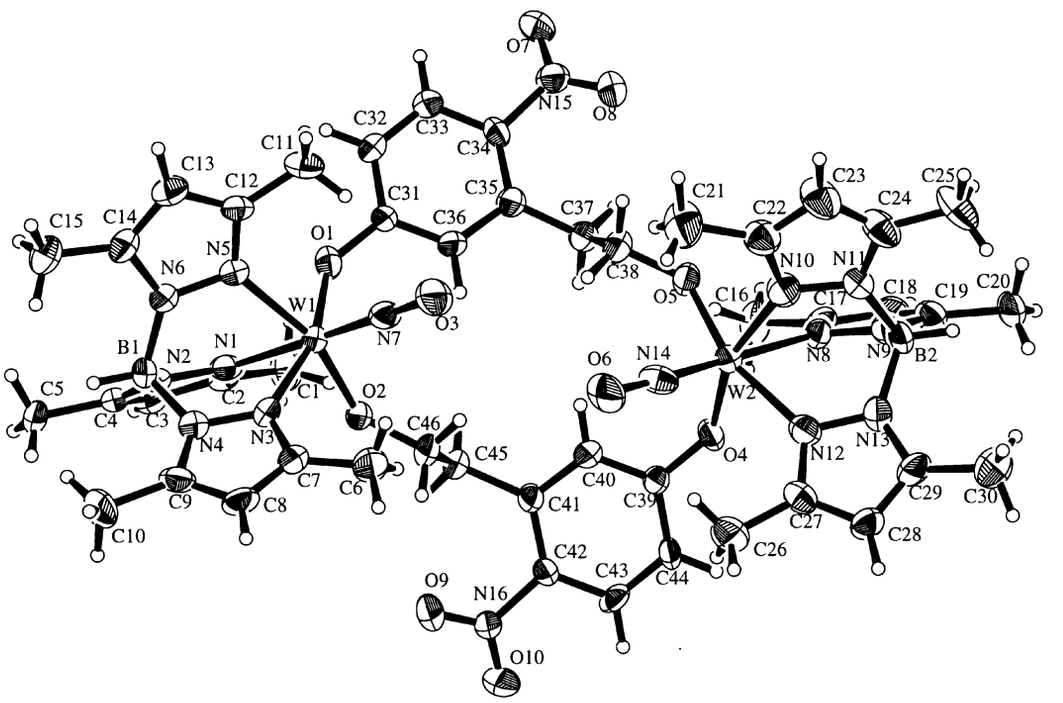

Fig. 6 A view of complex **15** showing the atom numbering.

Table 3 Crystallographic data for complexes **7** and **15**

	7	**15**
Formula	$C_{46}H_{60}B_2Mo_2N_{14}O_6 \cdot 2CH_2Cl_2$	$C_{46}H_{58}B_2N_{16}O_{10}W_2 \cdot CH_2Cl_2$
M	1288.4	1469.3
Crystal system	Monoclinic	Monoclinic
Space group	$P2_1/c$	$P2_1/c$
a/Å	14.730(3)	12.489(4)
b/Å	17.167(3)	24.166(9)
c/Å	24.701(5)	20.568(11)
β/°	106.55(2)	92.82(2)
V/Å^3	5987(2)	6200(5)
Z	4	4
T/°C	21	21
λ/Å	0.7107	0.7107
μ(MoKα)/mm^{-1}	0.654	3.857
$R_w(F_o^2)$	0.1507	0.1669
$R(F_o)$ for obs. reflections	0.0562	0.0583

rings, which competes with the oxygen-to-metal p_π–d_π donation. A similar effect had been noted previously.[11e]

The overall conformation of complexes **7** and **15** can be described by reference to the 12-atom best plane through the four oxygen atoms bonded to the metal, the methylene carbon atoms linking O(2) and O(5) to the phenyl rings, and the four linking atoms of the phenyl rings. In **7** this grouping is coplanar to within 0.96 Å, with the Mo atoms close to the plane, deviations 0.15 and 0.01 Å, and the nitrosyl oxygen atoms displaced by 2.93 and 2.87 Å on the same side of this central plane. The corresponding 12-atom grouping in **15** is somewhat more planar, with atomic deviations of up to to 0.69 Å, the W atoms are displaced by 1.44 and 1.39 Å and the nitrosyl oxygens by 3.23 and 3.16 Å on the same side of this plane. However, because of the difference in the linkages to the phenyl rings, the orientations of the M(NO)Tp^{Me2} residues relative to the central plane differs in the two complexes, as shown in Figs. 5 and 6. Thus the distance between the nitrosyl oxygen atoms is 7.15 Å in **7**, but only 3.70 Å in **15**. The corresponding metal to metal

Table 4 Selected geometrical parameters (distances in Å, angles in °) for complex **7**[a]

Mo(1)–N(1)	2.231(5)	Mo(2)–N(8)	2.238(6)
Mo(1)–N(3)	2.223(5)	Mo(2)–N(10)	2.211(5)
Mo(1)–N(5)	2.229(5)	Mo(2)–N(12)	2.207(6)
Mo(1)–N(7)	1.747(5)	Mo(2)–N(14)	1.764(5)
Mo(1)–O(1)	1.929(4)	Mo(2)–O(4)	1.919(4)
Mo(1)–O(2)	1.893(4)	Mo(2)–O(5)	1.897(4)
N(7)–O(3)	1.217(6)	N(14)–O(6)	1.204(6)
O(1)–C(31)	1.361(7)	O(4)–C(39)	1.358(7)
O(2)–C(46)	1.425(7)	O(5)–C(38)	1.427(7)
N(1)–Mo(1)–N(3)	84.1(2)	N(8)–Mo(2)–N(10)	85.0(2)
N(1)–Mo(1)–N(5)	83.2(2)	N(8)–Mo(2)–N(12)	85.0(2)
N(1)–Mo(1)–N(7)	175.2(2)	N(8)–Mo(2)–N(14)	179.8(2)
N(1)–Mo(1)–O(1)	83.2(2)	N(8)–Mo(2)–O(4)	81.4(2)
N(1)–Mo(1)–O(2)	85.0(2)	N(8)–Mo(2)–O(5)	83.4(2)
N(3)–Mo(1)–N(5)	78.9(2)	N(10)–Mo(2)–N(12)	77.0(2)
N(3)–Mo(1)–N(7)	92.6(2)	N(10)–Mo(2)–N(14)	94.9(2)
N(3)–Mo(1)–O(1)	162.6(2)	N(10)–Mo(2)–O(4)	161.7(2)
N(3)–Mo(1)–O(2)	89.8(2)	N(10)–Mo(2)–O(5)	88.9(2)
N(5)–Mo(1)–N(7)	92.8(2)	N(12)–Mo(2)–N(14)	95.1(2)
N(5)–Mo(1)–O(1)	87.8(2)	N(12)–Mo(2)–O(4)	89.6(2)
N(5)–Mo(1)–O(2)	164.5(2)	N(12)–Mo(2)–O(5)	162.5(2)
N(7)–Mo(1)–O(1)	99.3(2)	N(14)–Mo(2)–O(4)	98.8(2)
N(7)–Mo(1)–O(2)	98.4(2)	N(14)–Mo(2)–O(5)	96.4(2)
O(1)–Mo(1)–O(2)	100.9(2)	O(4)–Mo(2)–O(5)	101.6(2)
Mo(1)–N(7)–O(3)	175.3(5)	Mo(2)–N(14)–O(6)	178.1(5)
Mo(1)–O(1)–C(31)	135.6(4)	Mo(2)–O(4)–C(39)	141.7(4)
Mo(1)–O(2)–C(46)	132.8(4)	Mo(2)–O(5)–C(38)	130.2(4)
N(7)–Mo(1)–O(1)–C(31)	7.5(6)	N(14)–Mo(2)–O(4)–C(39)	5.7(5)
N(7)–Mo(1)–O(2)–C(46)	0.9(5)	N(14)–Mo(2)–O(5)–C(38)	−0.1(5)

[a] Values in parentheses are estimated standard deviations.

Table 5 Selected geometrical parameters (distances in Å, angles in °) for complex **15**[a]

W(1)–N(1)	2.204(12)	W(2)–N(8)	2.238(11)
W(1)–N(3)	2.149(12)	W(2)–N(10)	2.141(13)
W(1)–N(5)	2.181(11)	W(2)–N(12)	2.176(12)
W(1)–N(7)	1.741(12)	W(2)–N(14)	1.724(13)
W(1)–O(1)	1.942(9)	W(2)–O(4)	1.944(9)
W(1)–O(2)	1.873(8)	W(2)–O(5)	1.888(8)
N(7)–O(3)	1.224(14)	N(14)–O(6)	1.245(14)
O(1)–C(31)	1.365(14)	O(4)–C(39)	1.352(14)
O(2)–C(46)	1.432(15)	O(5)–C(38)	1.436(15)
C(34)–N(15)	1.501(17)	C(42)–N(16)	1.485(17)
N(15)–O(7)	1.189(14)	N(16)–O(9)	1.153(18)
N(15)–O(8)	1.202(15)	N(16)–O(10)	1.142(15)
N(1)–W(1)–N(3)	86.3(4)	N(8)–W(2)–N(10)	84.8(4)
N(1)–W(1)–N(5)	84.0(4)	N(8)–W(2)–N(12)	84.9(4)
N(1)–W(1)–N(7)	178.8(5)	N(8)–W(2)–N(14)	178.5(5)
N(1)–W(1)–O(1)	82.5(4)	N(8)–W(2)–O(4)	82.2(4)
N(1)–W(1)–O(2)	82.0(4)	N(8)–W(2)–O(5)	82.1(4)
N(3)–W(1)–N(5)	78.1(4)	N(10)–W(2)–N(12)	77.1(5)
N(3)–W(1)–N(7)	94.9(5)	N(10)–W(2)–N(14)	96.7(5)
N(3)–W(1)–O(1)	162.7(4)	N(10)–W(2)–O(4)	160.4(4)
N(3)–W(1)–O(2)	90.0(4)	N(10)–W(2)–O(5)	90.6(5)
N(5)–W(1)–N(7)	95.9(5)	N(12)–W(2)–N(14)	95.3(5)
N(5)–W(1)–O(1)	87.7(4)	N(12)–W(2)–O(4)	87.2(4)
N(5)–W(1)–O(2)	162.2(4)	N(12)–W(2)–O(5)	162.8(4)
N(7)–W(1)–O(1)	96.2(5)	N(14)–W(2)–O(4)	96.3(5)
N(7)–W(1)–O(2)	98.3(5)	N(14)–W(2)–O(5)	98.0(5)
O(1)–W(1)–O(2)	101.3(4)	O(4)–W(2)–O(5)	102.1(4)
W(1)–N(7)–O(3)	179.2(9)	W(2)–N(14)–O(6)	176.8(12)
W(1)–O(1)–C(31)	134.1(8)	W(2)–O(4)–C(39)	134.3(8)
W(1)–O(2)–C(46)	134.8(8)	W(2)–O(5)–C(38)	131.1(8)
N(7)–W(1)–O(1)–C(31)	19.5(12)	N(14)–W(2)–O(4)–C(39)	13.5(13)
N(7)–W(1)–O(2)–C(46)	2.4(13)	N(14)–W(2)–O(5)–C(38)	−1.0(12)

[a] Values in parentheses are estimated standard deviations.

distances are 8.63 and 7.77 Å. As noted previously,[11e] the central cavity of cyclic complexes of this type is generally too small to bind even small guest molecules. Critical cross-ring interatomic distances in **7** are C(35)···C(40) 3.59 and C(36)···C(41) 3.64 Å, with corresponding H···H distances, 3.13 and 3.26 Å, respectively. The central cavity of **15** is slightly larger, with C(36)···C(40) 4.68 Å and H36···H40 3.10 Å. Other short H···H distances, in the range 2.46–2.79 Å, are

between H36 and those bonded to C45 and C46, and between H40 and those bonded to C37 and C38. In addition the nitrosyl ligands block off one side of the cavity.

Crystals of both complexes contain solvent of crystallisation. Those of **7** contain two molecules of dichloromethane per complex molecule. The hydrogen atoms of one of these make contacts of 2.60 and 2.68 Å to ring oxygen atoms O(2) and O(5), respectively, of complex molecules separated by a unit cell translation along x, with angles C–H · · · O(2) and C–H · · · O(5) 148 and 150°. These distances are, however, too large to be considered as true hydrogen bonds, or at best only as exceedingly weak interactions.[19] The second dichloromethane appears to act as space filler and does not interact significantly with the complex molecule. In crystals of **15** there is one molecule of dichloromethane per complex molecule, in two sites, each with 50% occupancy. One of these "half molecules" is involved in a C–H · · · O interaction of 2.59 Å to nitrosyl oxygen atom O(6), with C–H · · · O angle of 143°. The other dichloromethane again appears to act as space filler.

Conclusion

The direct synthesis of metallomacrocycles from $[M(Tp^{Me2})(NO)I_2]$ and the unsymmetric ditopic ligands $HOC_6H_4(CH_2)_n$-OH-z (HE–E′H where $n = 1$, $z = 3$; $n = 2$, $z = 3$ or 4) is often, but not always, selective for the DL or *meso* isomers of $[M(Tp^{Me2})(NO)(E–E')]_2$ in preference to the *syn* or *anti* isomers. However, *syn* or *anti* isomers containing the $OC_6H_4CH_2O$-3 bridging ligand can be obtained using a stepwise synthesis involving reduction of $[M(Tp^{Me2})(NO)(OC_6H_4CHO\text{-}3)_2]$ prior to addition of the second metal centre. Since the *syn* or *anti* isomers do not readily convert into the DL or *meso* isomers it would appear that the reactions are kinetically controlled. The new metallomacrocycles are all redox active undergoing reduction processes at potentials which reflect the isomeric structure of the metallomacrocycle.

Acknowledgements

We are grateful to Mr M. Tolley and Mr P. R. Ashton for spectroscopic measurements. We also thank the EPSRC and the University of Birmingham for funds to purchase the R-Axis II diffractometer, and the EPSRC for supporting this work.

References

1 M. Fujita, J. Yazaki and K. Ogura, *J. Am. Chem. Soc.*, 1990, **112**, 5645; M. Fujita and K. Ogura, *Bull. Chem. Soc. Jpn.*, 1996, **69**, 1471; K. Birada, M. Aoyagi and M. Fujita, *J. Am. Chem. Soc.*, 2000, **122**, 2397; S. Y. Yu, T. Kusukawa, K. Birada and M. Fujita, *J. Am. Chem. Soc.*, 2000, **122**, 2665; K. Kasai, M. Aoyagi and M. Fujita, *J. Am. Chem. Soc.*, 2000, **122**, 2140.

2 P. J. Stang and B. Olenyuk, *Acc. Chem. Res.*, 1997, **30**, 502; J. Fan, J. A. Whiteford, B. Olenyuk, M. D. Levin, P. J. Stang and E. B. Fleischer, *J. Am. Chem. Soc.*, 1999, **121**, 2741; S. Leininger, P. J. Stang and B. Olenyuk, *Chem. Rev.*, 2000, **100**, 853.

3 J.-M. Lehn, *Supramolecular Chemistry*, VCH Verlagsgesellschaft, Weinheim, 1995; P. W. N. Baxter, J.-M. Lehn, G. Baum and D. Fenske, *Chem. Eur. J.*, 1999, **5**, 102; A. M. Garcia, F. J. Romero-Salguero, D. M. Bassani, J.-M. Lehn, G. Baum and D. Fenske, *Chem. Eur. J.*, 1999, **5**, 1803; L. A. Cuccia, J.-M. Lehn, J. C. Homo and M. Schmutz, *Angew. Chem., Int. Ed.*, 2000, **39**, 233.

4 C. J. Jones, *Chem. Soc. Rev.*, 1998, **27**, 289; M. D. Ward, *Annu. Rep. Prog. Chem., Sect. A Inorg. Chem.*, 1998, **94**, 311.

5 A. C. Try, M. M. Harding, D. G. Hamilton and J. K. M. Sanders, *Chem. Commun.*, 1998, 723; A. Bilyk and M. M. Harding, *J. Chem. Soc., Chem. Commun.*, 1995, 1697; M. Fujita, S. Nagao and K. Ogura, *J. Am. Chem. Soc.*, 1995, **117**, 1649.

6 J. Padilla, D. Gatteschi and P. Chaudhuri, *Inorg. Chim. Acta*, 1997, **260**, 217; J. Padilla, D. Gatteschi, P. Chaudhuri, I. Karpenstein, M. Winter, M. Lengen, C. Butzlaff, E. Bill, A. X. Trautwein, U. Flörke and H.-J. Haupt, *Inorg. Chem.*, 1993, **32**, 888.

7 M. H. Keefe, R. V. Slone, J. T. Hupp, K. F. Czaplewski, R. Q. Snurr and C. L. Stern, *Langmuir*, 2000, **16**, 3964; S. Belanger, J. T. Hupp, C. L. Stern, R. V. Slone, D. F. Watson and T. G. Carrell, *J. Am. Chem. Soc.*, 1999, **121**, 557; K. D. Benkstein, J. T. Hupp and C. L. Stern, *J. Am. Chem. Soc.*, 1998, **120**, 12982; R. V. Slone and J. T. Hupp, *Inorg. Chem.*, 1997, **36**, 5422; R. V. Slone, D. I. Yoon, R. M. Calhoun and J. T. Hupp, *J. Am. Chem. Soc.*, 1995, **117**, 11813.

8 D. W. Stephan, *Organometallics*, 1990, **9**, 2718.

9 A. W. Maverick and F. E. Klavetter, *Inorg. Chem.*, 1984, **23**, 4129; A. W. Maverick, S. C. Buckingham, Q. Yao, J. R. Bradbury and G. G. Stanley, *J. Am. Chem. Soc.*, 1986, **108**, 7430.

10 R. W. Saalfrank, N. Löw, S. Trummer, G. M. Sheldrick, M. Teichert and D. Stalke, *Eur. J. Inorg. Chem.*, 1998, 559.

11 (*a*) F. S. McQuillan, H. Chen, T. A. Hamor, C. J. Jones and K. Paxton, *Inorg. Chem.*, 1997, **36**, 4458; (*b*) F. S. McQuillan, H. Chen, T. A. Hamor and C. J. Jones, *Polyhedron*, 1996, **15**, 3909; (*c*) H. A. Hinton, H. Chen, T. A. Hamor, C. J. Jones, F. S. McQuillan and M. S. Tolley, *Inorg. Chem.*, 1998, **37**, 2933; (*d*) F. S. McQuillan, T. E. Berridge, H. Chen, T. A. Hamor, K. Paxton and C. J. Jones, *Inorg. Chem.*, 1998, **37**, 4959; (*e*) F. S. McQuillan, H. Chen, T. A. Hamor, C. J. Jones, H. A. Jones and R. P. Sidebotham, *Inorg. Chem.*, 1999, **38**, 1555; (*f*) N. AlObaidi, T. A. Hamor, C. J. Jones, J. A. McCleverty and K. Paxton, *J. Chem. Soc., Dalton Trans.*, 1987, 1063; (*g*) B. J. Coe, T. A. Hamor, C. J. Jones, J. A. McCleverty, D. Bloor, D. G. H. Cross and T. L. Axon, *J. Chem. Soc., Dalton Trans.*, 1995, 673.

12 S. J. Reynolds, C. F. Smith, C. J. Jones, J. A. McCleverty, D. C. Bower and J. L. Templeton, *Inorg. Synth.*, 1985, **23**, 4.

13 (*a*) TEXSAN, Single Crystal Analysis Software, version 1.6, Molecular Structure Corporation, The Woodlands, TX, 1993; (*b*) G. M. Sheldrick, SHELXL 93, Program for Crystal Structure Refinement, University of Göttingen, 1993; (*c*) C. K. Johnson, ORTEP, Report ORNL-5138, Oak Ridge National Laboratory, Oak Ridge, TN, 1976.

14 C. J. Jones, J. A. McCleverty, B. D. Neaves, S. J. Reynolds, H. Adams, N. A. Bailey and G. Denti, *J. Chem. Soc., Dalton Trans.*, 1986, 733.

15 S. M. Charsley, C. J. Jones, J. A. McCleverty, B. D. Neaves, S. J. Reynolds and G. Denti, *J. Chem. Soc., Dalton Trans.*, 1988, 293; S. M. Charsley, C. J. Jones, J. A. McCleverty, B. D. Neaves and S. J. Reynolds, *Transition Met. Chem.*, 1986, **11**, 329; S. M. Charsley, C. J. Jones, J. A. McCleverty, B. D. Neaves and S. J. Reynolds, *J. Chem. Soc., Dalton Trans.*, 1988, 301.

16 J. A. Thomas, M. G. Hutchings, C. J. Jones and J. A. McCleverty, *Inorg. Chem.*, 1996, **35**, 289.

17 N. AlObaidi, M. Chaudhury, D. Clague, C. J. Jones, J. C. Pearson, J. A. McCleverty and S. S. Salam, *J. Chem. Soc., Dalton Trans.*, 1987, 1733.

18 N. J. AlObaidi, S. S. Salam, P. D. Beer, C. D. Bush, T. A. Hamor, F. S. McQuillan, C. J. Jones and J. A. McCleverty, *Inorg. Chem.*, 1992, **31**, 263.

19 W. C. Hamilton and J. A. Ibers, *Hydrogen Bonding in Solids*, W. A. Benjamin, Inc., New York, 1968, pp. 182–183; R. Taylor and O. Kennard, *J. Am. Chem. Soc.*, 1982, **104**, 5063; G. R. Desiraju, *Acc. Chem. Res.*, 1991, **24**, 290; T. J. Steiner, *Chem. Commun.*, 1997, 727.